Experiments in Fluids 36 (2004) 419–421
DOI 10.1007/s00348-003-0739-1

Turbulent Taylor-Couette vortex flow between large radius ratio concentric cylinders

W. M. J. Batten, S. R. Turnock, N. W. Bressloff, S. M. Abu-Sharkh

Abstract Turbulent Taylor vortices between two concentric cylinders have been studied at a very high radius ratio of 0.985, equivalent to that found in relatively small underwater thruster units (typically with gaps of 2 mm). In order to study the flow at this radius ratio, a 1.42-m diameter experimental apparatus (with a rotating inner cylinder and a stationary outer cylinder) was constructed possessing a gap of 10 mm. Consequently, air bubbles could be visualised translating in water. A method was developed for identifying Taylor vortex properties from filtered digital images of the air bubbles and summing intensities to produce bubble density distributions. Whereas individual instantaneous images can be misleading, averaged bubble density distributions make it possible to identify vortex separation sizes and the positions of vortex outflow boundaries.

1 Introduction

The flow between a rotating inner cylinder and a fixed outer cylinder (Taylor-Couette flow), first reported by Taylor (1923), is of interest in several engineering applications, such as motors, filters, pumps, and journal bearings. The motivation for the work presented here stemmed from the development of a novel underwater-integrated electrical thruster unit (Abu-Sharkh et al. 2003), in which a significant source of power loss arises due to the frictional resistance that occurs between the rotor and the stator.

The majority of Taylor-Couette experimental facilities reported in the literature operate with radius ratios, $\eta=R_1/R_2$ (where the outer radius, R_2, is the sum of the inner radius, R_1, and the gap, d), in the range $0.6<\eta<0.95$. However, many engineering applications (including the thruster unit above) involve much smaller clearance ratios in which $0.95<\eta<1$. Hence, for this investigation an experimental rig was designed to be dynamically similar to the thruster unit, $\eta=0.985$. This required the gap to be scaled from 2 to 10 mm to produce an environment in which flow visualisation could be conducted. The resulting apparatus has an inner cylinder radius of 710 mm. Further details of the experimental setup can be found in Batten (2002).

An inexpensive flow visualisation procedure was developed involving filtered digital images of air bubbles in water with the aim of capturing the position and extent of the turbulent Taylor vortices found at the operating condition of the thrusters, given by the Taylor number

$$Ta = Re^2 \frac{d}{R_1} = 10^7$$

and the Reynolds number based on gap width

$$Re = \frac{Ud}{\nu} = 29400$$

where U signifies the speed of the inner cylinder and ν denotes the kinematic viscosity.

When using bubbles in Taylor-Couette flow, they are subjected to forces due to pressure differences, flow momentum, buoyancy, drag, and gravity. Evidence suggests (Atkhen et al. 2000; Djeridi et al. 2002) that pressure forces dominate since bubbles accumulate adjacent to the rotor in the vicinity of the outflow corresponding to regions of low pressure. Hence, the aim here was to demonstrate such an accumulation of bubbles and use this to determine the mean locations of Taylor cells.

2 Analysis and discussion

For this investigation, the bubble trajectories and locations were recorded using a digital video camera (Panasonic, type NV-DS15) with 800 kbytes image resolution and 100 images were saved at 0.5-ms intervals. Two typical images are shown in Fig. 1. The whole length of the inner cylinder is clearly visible, although the base is slightly obscured due to reflection of the base of the window. Importantly, while the bubble trajectories are observed to be close to the inner cylinder, distinct regions of bubble clustering are less obvious throughout both images.

Thus, in order to better understand the bubble pattern in these experiments and produce a map of bubble densities along the length of the inner cylinder the images were analysed numerically. The raw bubble images were cropped to the size of the gap, converted to a grey scale negative, and then filtered to a specific grey scale threshold to remove the background leaving only images of bubbles.

Received: 11 April 2002 / Accepted: 19 September 2003
Published online: 28 November 2003

W. M. J. Batten, S. R. Turnock, N. W. Bressloff (✉), S. M. Abu-Sharkh
School of Engineering Sciences,
University of Southampton,
Southampton, SO17 3BJ, UK
E-mail: nwb@soton.ac.uk
Tel.: +44-2380-595473
Fax: +44-2380-594813

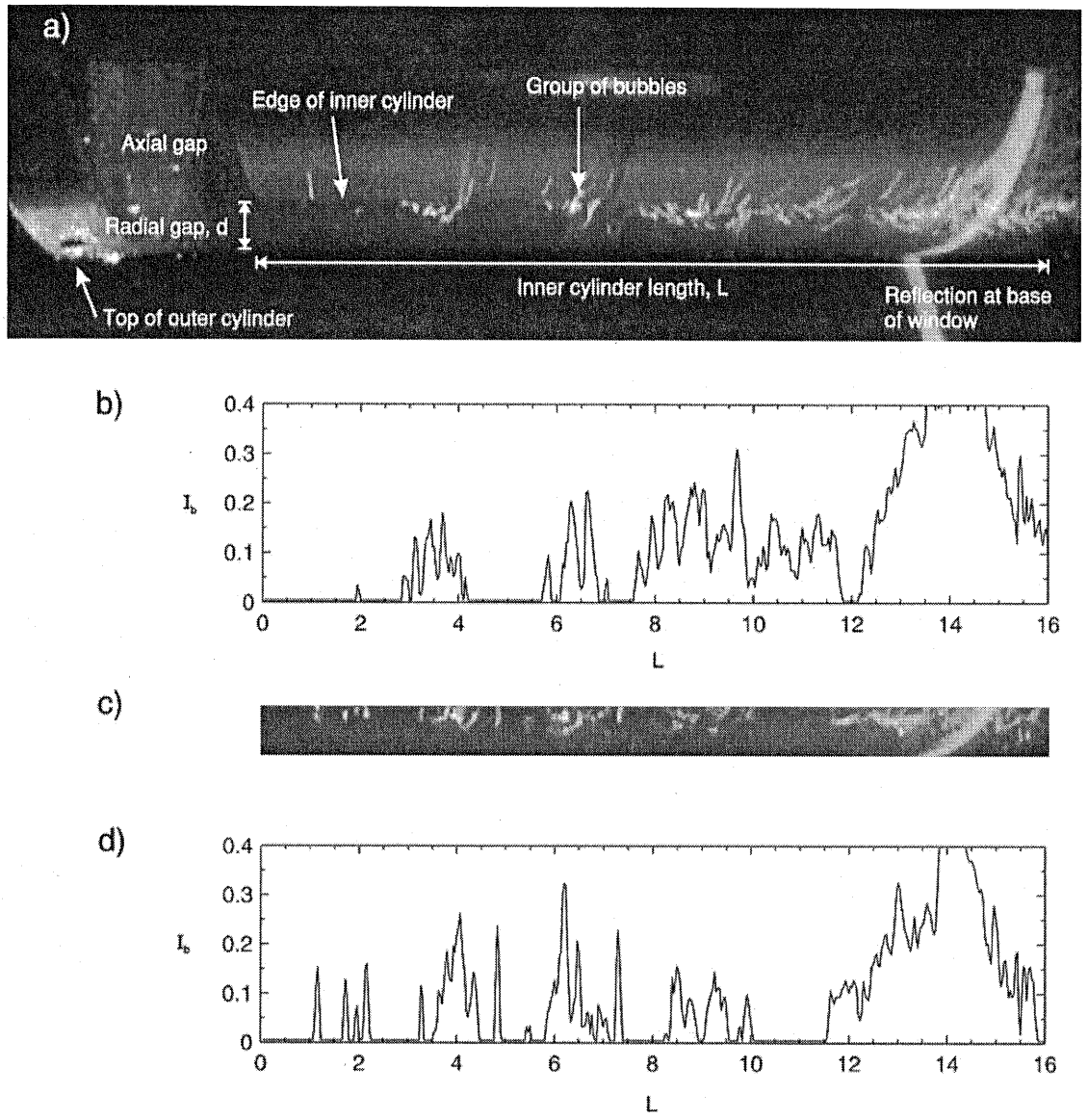

Fig. 1. Instantaneous bubble distribution densities 0.5 ms apart for *Re*=29,400. **a** Raw image showing poorly defined clustering of bubble trajectories; **b** Bubble density distribution for image in **a**; **c** Cropped raw image 0.5 ms later than in **a** showing a better defined clustering of bubble trajectories; **d** Bubble density distribution for image in **c**

Altering the threshold level had little effect on the overall pattern but helped to remove noise produced by background light. The bubble distributions were then computed along the length by summing grey scales across the gap and scaling to yield a non-dimensionalised density distribution, I_b, such that I_b=1 would represent a line of bubbles across the gap.

This procedure is demonstrated in Fig. 1. A complete set of these images is presented in Batten (2002). Fig. 1a and c show raw photographic images of the flow 0.5 ms apart. Note that these images have been rotated 90° anticlockwise: the base of the inner cylinder is on the right, where reflection produced overly strong light intensity of the bubbles in this region, and the upper edge of the inner cylinder is evident and aligned with the digitised images in Fig. 1b and d. Unsurprisingly, the digitised images do not reveal more about the flow than can be ascertained from studying the raw images. This includes the lack of definition of bubble trajectory clustering in the lower half of the flow in Fig. 1a. Thus, it is clear that significant differences exist in these instantaneous images and a time-averaged bubble density distribution, $\bar{I}_b$, should be assessed for this turbulent flow.

Such an average is shown in Fig. 2 for 100 images and the locations of high bubble density are clearly depicted. Assuming that, under these flow conditions, the accumulation of bubbles near the outflow adjacent to the rotor corresponds to regions of low pressure, the procedure

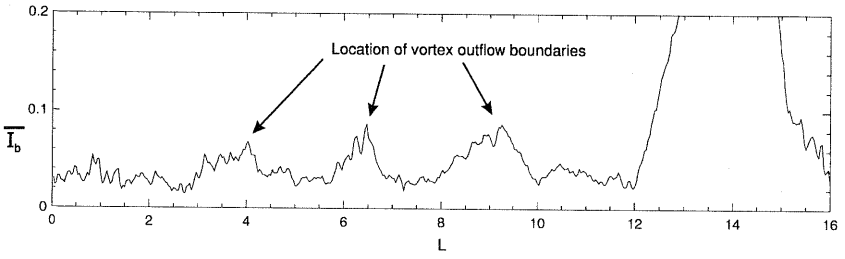

Fig. 2. Time-averaged bubble density distribution for *Re*=29,400

identifies the mean locations of vortex outflows and the associated Taylor cells.

In conclusion, in this article we have (1) presented flow visualisation of turbulent Taylor-Couette flow in a very high radius ratio annulus and (2) demonstrated the effectiveness of a relatively straightforward and inexpensive means for capturing important mean flow features that are not easily identifiable from instantaneous images. We now intend to investigate the effect of modifications to the gap geometry and axial flow in this large radius ratio device, both in terms of the Taylor-Couette flow and the associated frictional losses. Also, in order to improve the quality of bubble tracking, seeded hydrogen bubbles and a higher resolution camera will be used.

References

Atkhen K, Fontaine J, Westfreid JE (2000) Highly turbulent Couette-Taylor bubbly flow patterns. J Fluid Mech 422:55–68

Batten WMJ (2002) Numerical predictions and experimental analysis of small clearance ratio Taylor-Couette flows. PhD thesis, School of Engineering Sciences, University of Southampton, UK

Djeridi H, Gabillet C, Billard JY (2002) Two phase Couette Taylor flow. C R Mec 330(2):113–119

Abu-Sharkh SM, Turnock SR, Hughes AW (2003) Design and performance of an electric tip-driven thruster. Proc Inst Mech Eng Part M 217:1–15

Taylor GI (1923) Stability of a viscous liquid contained between two rotating cylinders. Trans R Soc London A 233:289–343